Journal of Crystal Growth 425 (2015) 25–28

Contents lists available at ScienceDirect

Journal of Crystal Growth

journal homepage: www.elsevier.com/locate/jcrysgro

Control of anion incorporation in the molecular beam epitaxy of ternary antimonide superlattices for very long wavelength infrared detection

H.J. Haugan [a,*], G.J. Brown [a], S. Elhamri [b], L. Grazulis [a]

[a] Air Force Research Laboratory, Materials and Manufacturing Directorate, Wright-Patterson Air Force Base, Ohio 45433, United States
[b] Department of Physics, University of Dayton, Ohio 45469, United States

ARTICLE INFO

Available online 17 March 2015

Keywords:
A3. Superlattices
A3. Molecular beam epitaxy
B1. Antimonides
B3. Infrared detector

ABSTRACT

Authors discuss how anion incorporation was controlled during the epitaxial growth process to develop InAs/GaInSb superlattice (SL) materials for very long wavelength infrared applications. A SL structure of 47.0 Å InAs/21.5 Å $Ga_{0.75}In_{0.25}Sb$ was selected to create a very narrow band gap. Although a molecular beam epitaxy growth developed can produce a strain balanced ternary SL structure with a precisely controlled band gap around 50 meV, the material quality of grown SL layers is particularly sensitive to growth defects formed during an anion incorporation process. Since Group III antisites are the dominant structural defects responsible for the low radiative efficiencies, the authors focus on stabilizing III/V incorporation during SL layer growth by manipulating the growth surface condition for a specific anion cracking condition. The optimized ternary SL materials produced an overall strong photoresponse signal with a relatively sharp band edges and a high mobility of ~10,000 $cm^2/V\,s$ that is important for developing infrared materials.

1. Introduction

The InAs/GaInSb superlattice (noted as "ternary SL") system provides several distinctive theoretical advantages suitable for very long wavelength infrared (VLWIR) detection [1]. With increasing indium composition, a very narrow band gap can be achieved with a smaller period for the ternary SL system, leading to a larger absorption coefficient due to enhanced electron and hole wavefunction overlap [2]. More importantly, the strain can create a large splitting between the heavy-hole and light-hole bands in the ternary SLs, which reduces the hole–hole Auger recombination process and increases the minority carrier lifetime, thus improving the device detectivity. Based on minimizing the Auger recombination, Grein et. al. [3] proposed a strain balanced VLWIR ternary SL of 47.0 Å InAs/21.5 Å $Ga_{0.75}In_{0.25}Sb$, which is the design used in our studies. Haugan et al. [4,5] have shown improvements in the quality of the ternary materials produced using molecular beam epitaxy (MBE) growth process for this design. Their optimized SL materials produced a strong photoresponse signal, a high mobility, and a long 300 K carrier lifetime. Although longer carrier lifetimes have been reported in mid-wave InAs/InAsSb (noted as "Ga-free) SLs [6], unfortunately to strain balance these Ga-free SLs in a VLWIR design requires a much wider period, ~147 Å [7] versus the 68.5 Å used in this study, significantly impacting the absorption coefficient. Therefore, the ternary SL materials are still important for VLWIR detection.

In this work, using a combination of high-resolution X-ray diffraction (HRXRD), atomic force microscopy (AFM), temperature-dependent Hall (TdH) effect, and photoconductivity measurements, we continuously refined the MBE process and tuned growth conditions to produce high-quality ternary SL materials to be used for VLWIR detection. Since most MBE-grown III–V heterostructures are affected by a large number of growth defects generated during the III–V surface reconstruction process, we optimized the III/V stoichiometry by manipulating the growth surface condition such as anion fluxes, Sb cracking condition, and growth temperature. We used a SL structure of 47.0 Å InAs/21.5 Å $Ga_{0.75}In_{0.25}Sb$ to create the band gap around 50 meV.

2. Ternary superlattice growths

The InAs/GaInSb SL materials in this study were grown in a Varian MBE reactor equipped with dual-filament effusion cells for the Group III elements, and valved cracker cells for the Group V elements. The repeated SL stacks (0.5 μm-thick) and the undoped

* Corresponding author.
E-mail address: heather.haugan.ctr@us.af.mil (H.J. Haugan).

http://dx.doi.org/10.1016/j.jcrysgro.2015.03.008
0022-0248/

GaSb buffer layer (0.5 μm-thick) were deposited on GaSb (100) wafers, and several series of 47.0 Å InAs/21.5 Å $Ga_{0.75}In_{0.25}Sb$ SL samples were grown over a wide range of anion flux conditions to preset the growth rates of Group III elements and the V/III flux ratio. To grow the intended ternary structure under minimum cross contamination environment of the anion fluxes, the V/III beam equivalent pressure (BEP) ratio was set at ~3 for both GaInSb and InAs layer depositions and the growth rates of 1.6 and 0.3 Å/s were used for GaInSb and InAs layers, respectively. The Sb cracking zone temperature was varied between 850 and 1000 °C in order to investigate the III-Sb incorporation during a growth, while the As cracking zone temperature was set at 900 °C. Fig. 1 shows a typical strain-balanced ternary structure with an excellent crystalline quality that can be achieved by using the shutter sequence described in the inset of Fig. 1. With measured period of 68.0 Å, the grown structure produced a band gap of 53 meV, or a corresponding onset wavelength of 23 μm, as demonstrated in the photoresponse (PR) spectrum in Fig. 2.

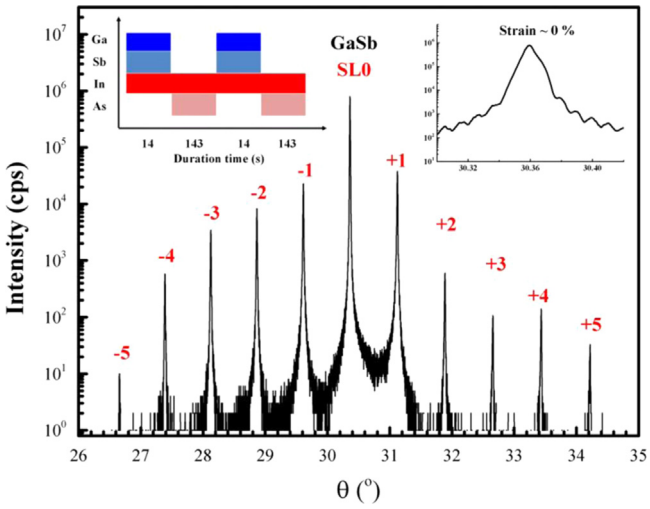

Fig. 1. X-ray diffraction patterns of a 68.0 Å period superlattice (SL) sample containing a 0.5 μm thick 47.0 Å InAs/21.5 Å $Ga_{0.75}In_{0.25}Sb$ SLs. Inset is the shutter sequence employed to create a strain-balanced ternary structure.

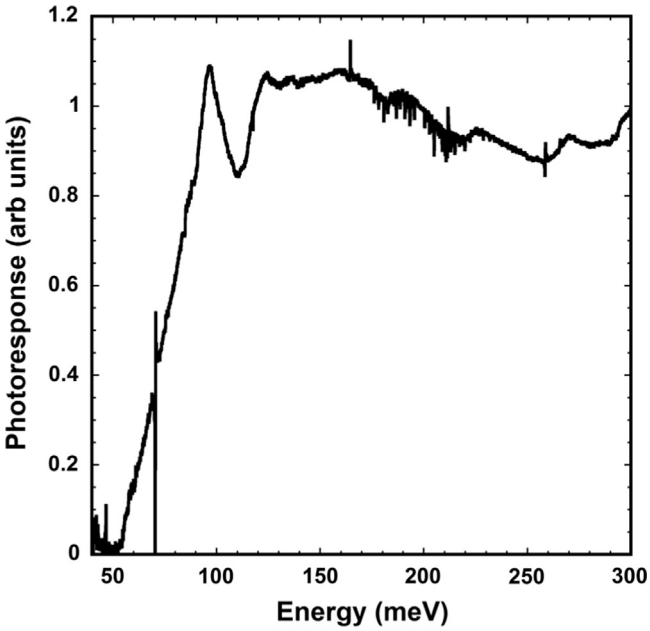

Fig. 2. Photoresponse spectrum at 10 K for the 47.0 Å InAs/21.5 Å $Ga_{0.75}In_{0.25}Sb$ superlattices.

3. Results and discussions

In order to stabilize the III-Sb incorporation, a comparative deposition temperature (T_g) study was performed using various Sb cracking conditions to generate beams of tetramers, dimers, and monomers. Although some studies showed that a nearly 100% yield of Sb monomers can be achieved at a cracker temperature above ~1100 °C [8,9], no systematic study has been done to determine Sb mole fraction as a function of cracker temperature for our EPI Model 200 cc Mark V Corrosive Series Valved Cracker. Since the most obvious effect one would expect from a III/V ratio not equal to one is morphological disorder induced by the nucleation of surface defects, we used 50 μm × 50 μm area scans by AFM to monitor surface roughness as a function of the T_g. For a series of samples grown under a low Sb cracking condition (Sb cracker temperature of 850 °C), the SL roughens very quickly as the T_g is increased above 420 °C. Fig. 3 top shows the apparent surface damage observed by AFM for the sample grown at the highest T_g of 440 °C. The root-mean-square (RMS) value quickly changes from 2 to 61 Å as the T_g increases from 420 to 430 °C and further increases up to 80 Å at higher temperatures highlighting the noticeable surface damage that occurred at 430 °C and above. While the exact surface pitting mechanism is undetermined, it is common to see pitted surfaces in the SL layers grown under a metal-rich condition due to the higher desorption rate of anion fluxes at the growth surfaces [10].

To relate the observed surface pitting phenomena to the spectral response, low temperature photoconductivity measurements were performed and Fig. 4d plots their results. The PR spectra were collected with fourier transform infrared spectrometer over a wavelength range from 2 to 50 μm at a temperature of 10 K. Due to the relatively low resistivity of the samples, the photoconductivity was measured in the current-biased mode, with a current of 0.5 mA between two parallel strip contacts on the surface. The PR intensities in Fig. 4d were measured at 100 meV above the onset. Although these intensities are given in arbitrary units (a.u.), the relative signal strengths can still be compared as the test conditions for all the samples were kept constant. The typical band gap energies of SLs grown at the same low T_g were around 48 ± 5 meV. However for $T_g > 420$ °C, the band gap did increase, as listed in Table 1. The PR intensity gradually decreases from 1.07 to 0.8 a. u. as T_g increases from 410 to 420 °C, when SL layers were grown under low Sb cracking condition generating low fraction of Sb monomers. The result of much lower PR intensity for the samples deposited at high temperatures does follow the severe surface damage trend observed in AFM scans.

Although there is a variety of ways of controlling surface roughness, such as by increasing V/III flux ratio, we increased Sb cracker temperature to generate more Sb monomers to enhance III-Sb incorporation. For a series of samples grown under high Sb cracking condition (Sb cracker temperature of 950 °C), the SL layers were deposited without any noticeable surface defects at temperature as high as 470 °C. Fig. 4a plots the RMS values as a function of T_g from SL samples grown with the Sb cracker at 950 °C. In contrast to the AFM results observed in Fig. 3 top, there were no significant changes in the RMS roughness for the SL samples deposited at T_g between 410 and 450 °C, and the RMS values remained in a range of ~3 Å. Although there were no noticeable surface damages occurring at elevated temperatures (see Fig. 3 bottom), the PR signal strength was still affected by T_g. Fig. 4d indicates that the PR intensity gradually increases as T_g